Kinetic Reaction Scheme for the Dihydrofolate Reductase Domain of the Bifunctional Thymidylate Synthase−Dihydrofolate Reductase from *Leishmania major*†

Po-Huang Liang‡ and Karen S. Anderson*

Department of Pharmacology, Yale University School of Medicine, 333 Cedar Street, New Haven, Connecticut 06520-8066

Received February 9, 1998; Revised Manuscript Received June 18, 1998

ABSTRACT: In several species of protozoa, the catalytic activities for the enzymes dihydrofolate reductase (DHFR) and thymidylate synthase (TS) reside on a single polypeptide chain constituting a bifunctional thymidylate synthase−dihydrofolate reductase enzyme. In most other species, however, these enzymes occur as monofunctional catalytic activities on separate enzymes. In this study, the kinetic reaction scheme for the dihydrofolate reductase activity from the bifunctional thymidylate synthase−dihydrofolate reductase (TS−DHFR) isolated from the parasite *Leishmania major* is compared to that of the monofunctional DHFR purified from *Escherichia coli.* Examination using pre-steady-state kinetic methods reveals interesting differences between the bifunctional and monofunctional forms of the dihydrofolate reductase enzymes. The rate-limiting step in the kinetic pathway for the monofunctional *E. coli* enzyme is the release of product, tetrahydrofolate. In contrast, for the *L. major* bifunctional enzyme, the kinetic step which limits the steady-state turnover is a conformational change associated with the release of $NADP^+$. A complete kinetic description for the dihydrofolate reductase reaction pathway for the bifunctional enzyme is presented.

Dihydrofolate reductase (DHFR)[1] catalyzes the reduction of dihydrofolate (H_2folate) by NADPH to generate tetrahydrofolate (H_4folate) which is required for transfer of one carbon unit in several biochemical processes, including the biosynthesis of thymidylate, purines, and amino acids. Therefore, dihydrofolate reductase has been intensively investigated as a target for anticancer and antibacterial drugs. The three-dimensional structure and reaction kinetic pathway for dihydrofolate reductases from a number of species have been determined. The DHFR from *Escherichia coli* is perhaps the most well-studied member of this protein family. In the *E. coli* DHFR, it has been established that the substrates (H_2folate and NADPH) bind to DHFR in a random order (*1*, *2*) and that the binding between cofactor and folate is synergistic (*3*). The steady-state turnover rate of the preferred kinetic pathway at low pH is limited by the dissociation of H_4folate from the E·NADPH·H_4folate ternary complex. This complex is formed upon displacement of $NADP^+$ in the E·$NADP^+$·H_4folate by NADPH (*4*). At high pH, the hydride transfer of NADPH becomes the rate-limiting step (*4*). The pH dependence of the steady-state rate shows an apparent pK_a of 8.4 due to a change in the rate-limiting step (*4*).

Scheme 1

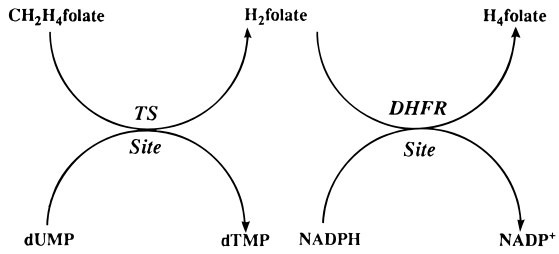

A unique family of DHFR reductase enzymes have been isolated from several parasitic protozoan species, including *Leishmania*, *Toxoplasma gondii*, and *Cryptosporidium* (*5*, *7*, *22*−*24*). Collectively, these parasite pathogens cause many of the opportunistic infections in individuals infected with the HIV-1 virus (*22*). These opportunistic infections often signal the first indication of the clinical AIDS syndrome and moreover represent the primary cause of suffering and death. To effectively treat these AIDS patients who are suffering from these opportunistic infections, enzymes which are unique to parasites are likely to provide viable targets for the design of novel antiparasitic drugs.

In these protozoan species, the DHFR is found on a single polypeptide chain with thymidylate synthase (TS) as illustrated in Scheme 1. The thymidylate synthase catalyzes the conversion of deoxyuridine monophosphate (dUMP) and (6*R*)-L-5,10-methylene tetrahydrofolate (CH_2H_4folate) to deoxythymidine monophosphate (dTMP) and H_2folate. TS and DHFR are the sequential enzymes in the de novo synthesis of dTMP. The monofunctional DHFR exists as a monomer in its native state with a molecular mass of approximately 20 kDa. The bifunctional TS−DHFRs are

† This work was supported by NIH Grants GM45353 and GM49551 to K.S.A.

* To whom correspondence should be addressed. Telephone: (203) 785-4526. Fax: (203) 785-7670. E-mail: karen.anderson@yale.edu.

‡ Present address: Department of Macromolecular Science, SmithKline Beecham, 709 Swedeland Rd., King of Prussia, PA 19406.

[1] Abbreviations: TS, thymidylate synthase; DHFR, dihydrofolate reductase; CH_2H_4folate, methylene tetrahydrofolate; H_4folate, tetrahydrofolate; H_2folate, dihydrofolate; MTX, methotrexate. All other abbreviations are those recommended by IUPAC.

S0006-2960(98)00317-1 CCC: $15.00
Published on Web 08/11/1998

much larger, having native molecular masses ranging from 100 to 240 kDa (*6*, *9*). The TS−DHFR from *Leishmania major* has been shown to be a dimer with a subunit molecular mass of 58 kDa, and the three-dimensional structure has recently been solved (*7*, *8*). The three-dimensional structures of the bifunctional TS−DHFR domains are similar to the individual monofunctional TS and DHFR structures. However, the DHFR domain of the bifunctional enzyme has an N-terminal extension consisting of 22 additional amino acids which winds along a shallow channel on the surface of the TS domain of that subunit (*8*).

Steady-state kinetic studies have been conducted on the bifunctional TS−DHFR enzyme (*5*). Although a complete kinetic scheme for the dihydrofolate reductase reaction pathway is available for the monofunctional *E. coli* and human enzymes (*4*, *10*), an in-depth kinetic and thermodynamic description of the DHFR pathway for a bifunctional enzyme has not been carried out. In this study, we use a rapid transient kinetic approach utilizing stopped-flow fluorescence in conjunction with equilibrium fluorescence methods to construct the kinetic reaction pathway for the DHFR domain of bifunctional TS−DHFR. In addition, we address the similarities and differences between the kinetic reaction pathways for the DHFR catalytic activity for monofunctional and bifunctional DHFR enzymes. A detailed mechanistic evaluation of the bifunctional DHFR, including kinetic distinctions from the monofunctional DHFR, may provide crucial information that may be exploited as a novel therapeutic approach.

MATERIALS AND METHODS

Enzyme. A clone harboring the pO2CLSA-4 plasmid expressed in an *E. coli* Rue 10 expression vector was used along with previously described methods to obtain protein of high purity (*11*, *12*, *21*). The purified protein has both thymidylate synthase and dihydrofolate reductase activities similar to those previously reported bifunctional forms of the enzyme (*5*, *11*, *12*).

Chemicals. All buffers and other reagents employed were of the highest commercial purity. Millipore ultrapure water was used for all solutions. Dihydrofolate (H_2folate) was chemically prepared from the reduction of folate by sodium hydrosulfite (*13*). Tetrahydrofolate (H_4folate) was enzymatically prepared from H_2folate by using *E. coli* DHFR (*14*). Both compounds were purified using DE-52 anion exchange resin and elution with a linear gradient of triethylammonium bicarbonate (*15*). The concentration of H_2folate was determined using a molar extinction coefficient of 28 000 M^{-1} cm^{-1} at 282 nm (*16*). The concentration of H_4folate was determined by using a molar extinction coefficient of 28 000 M^{-1} cm^{-1} at 297 nm (*17*). NADPH was purchased from Sigma, and its concentration was determined by using a molar extinction coefficient of 6220 M^{-1} cm^{-1} at 340 nm. All stopped-flow fluorescence experiments were carried out at 25 °C in either 50 mM Tris buffer (pH 7.8) containing 10 mM dithiothreitol (DTT) (buffer A) in which TS maintains its full activity or buffer B (pH 7.8) containing 50 mM 2-(*N*-morpholino)ethanesulfonic acid, 25 mM tris(hydroxymethyl)-aminoethane, 25 mM ethanolamine, and 100 mM sodium chloride (MTEN buffer) with 1 mM DTT previously used for the purpose of comparison (*4*). The buffer solutions were always purged with argon prior to being used.

Enzyme Assay. The DHFR activity of the bifunctional enzyme was determined by following the decrease in absorbance at 340 nm that accompanies the conversion of substrates NADPH and H_2folate to products $NADP^+$ and H_4-folate ($\Delta\epsilon = 12.8$ mM^{-1} cm^{-1}) as described previously (*5*).

Enzyme Concentration. The concentration of TS−DHFR was estimated spectrophotometrically at 280 nm by using a molar extinction coefficient of 67 800 M^{-1} cm^{-1}, a Bio-Rad assay, or active site titration using methotrexate (MTX) as a specific inhibitor for the DHFR domain. The active site concentration of the DHFR domain in the bifunctional TS−DHFR was determined by monitoring the decrease in intrinsic protein fluorescence upon titration with methotrexate (MTX). The enzyme concentrations determined from each of these methods were consistent.

Equilibrium Fluorescence Experiments. Steady-state measurements to determine the K_d for ligands at the DHFR site were performed using an SLM 4800 fluorimeter (Urbana, IL) at 25 °C as previously described (*18*, *21*). The data were fitted a quadratic expression which relates the observed fluorescence to the concentration of ligand and provides an estimate of the K_d (*18*).

Stopped-Flow Experiments. Stopped-flow measurements were performed using a Kintek SF-2001 apparatus (Kintek Instruments, State College, PA) as previously described (*21*). In the experiments designed to measure the dissociation rate constants shown in Table 3, the trapping ligand (L_2) was used at a concentration of >5-fold excess over that of L_1 to allow analysis as a pseudo-first-order rate constant. The data were collected over a given time interval by an IBM 486 computer using software provided by Kintek Instruments. Rate constants were obtained by fitting the data to a single or double exponential by nonlinear regression analysis.

RESULTS AND DISCUSSION

Equilibrium Fluorescence Measurements. The equilibrium dissociation constants (K_d) for H_2folate, NADPH, $NADP^+$, and H_4folate binding to the DHFR site of TS−DHFR were measured by monitoring the protein fluorescence quenching. The plot of protein fluorescence versus [L] was fit to a quadratic equation to obtain the K_d constants. The K_d values for different substrates at 25 °C and pH 7.8 (buffer A) are summarized in Table 1. A representative K_d titration curve for H_2folate with the bifunctional TS−DHFR enzyme is shown in Figure 1.

Table 1: Equilibrium Dissociation Constants for the DHFR Site of TS−DHFR at pH 7.8 and 25 °C

ligand	enzyme species	K_d (μM)
H_2folate	E	0.46 ± 0.03
NADPH	E	0.17 ± 0.02
H_4folate	E	0.016 ± 0.01
$NADP^+$	E·H_4folate	1.66 ± 0.07
$NADP^+$	E	1.24 ± 0.1
NADPH	E·H_4folate	0.49 ± 0.03

Kinetics of Ligand Binding. The second-order rate constants for the binding of substrates to the DHFR domain of the bifunctional TS−DHFR were determined by measuring the dependence of the observed rate on substrate concentration. The apparent first-order rates for H_2folate and NADPH were determined by using stopped-flow fluorescence by monitoring the quenching of intrinsic enzyme fluorescence

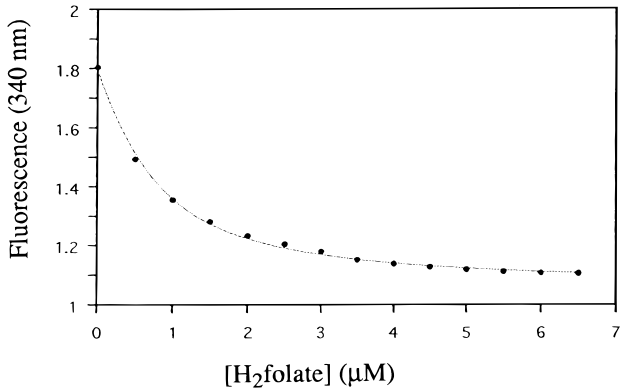

FIGURE 1: Equilibrium fluorescence titration to determine the K_d for the interaction of H_2folate with TS−DHFR. The decrease in intrinsic protein fluorescence was monitored as the ligand (H_2folate) was added in small increments (0.5 μL) to a solution of TS−DHFR (0.58 μM) until no further change was noted. The curve shows the best fit of the data of the quadratic equation which gives a K_d of 0.46 μM.

when they were mixed with ligand. A representative stopped-flow fluorescence trace for the binding of H_2folate to the bifunctional enzyme is shown in Figure 2A. In this experiment, the enzyme (0.29 μM) was mixed with H_2folate (5 μM). As illustrated in Figure 2A, the data are biphasic and fit to a double exponential with the first exponential rate of 187 ± 22 s^{-1} for the faster phase and 9 ± 0.46 s^{-1} for the second slower phase. Similar results were obtained for the binding of NADPH to enzyme. All measurements were conducted in buffer A (see Materials and Methods) for optimal TS enzymatic activity.

The binding of H_2folate to the *E. coli* monofunctional DHFR was examined under the same experimental conditions to provide a direct comparison with the bifunctional enzyme. Under the identical conditions, when the *E. coli* enzyme (0.29 μM) is mixed with H_2folate (5 μM), two exponential phases for binding are also observed, as illustrated in Figure 2B. The data fit a double exponential with a rate of 375 ± 60 s^{-1} for the faster phase and 44 ± 6 s^{-1} for the slower phase. Only the faster phase for either the bifunctional or monofunctional enzyme was dependent upon ligand concentration. Since the slower phase was independent of ligand concentration for both the bifunctional and monofunctional enzyme, this rate most likely represents a conformational change. This conformational change may correspond to the slow interconversion of two enzyme conformers, E and E_0 (one active and one inactive), as previously suggested for the *E. coli* monofunctional DHFR and illustrated in Scheme 2 (*3*). If this is indeed the case, then the putative interconversion between E_0 and E, after the binding of H_2folate, is slower for the bifunctional enzyme (9 s^{-1}) as compared with that of the monofunctional enzyme (44 s^{-1}). Thus, there is a 5-fold difference in the bifunctional and *E. coli* monofunctional DHFR enzyme conformer interconversion rates.

As indicated, only the first exponential phase (Figure 2A) was found to be dependent upon ligand concentration. The apparent first-order binding rate of the first exponential phase was found to be linearly dependent upon the concentration of substrate concentration and obey the equation $k_{obs} = k_{on}[L] + k_{off}$, in which k_{obs}, k_{on}, and k_{off} are the apparent first-order observed binding rate, association rate constant, and dissociation rate constant, respectively. Therefore, k_{on} is the

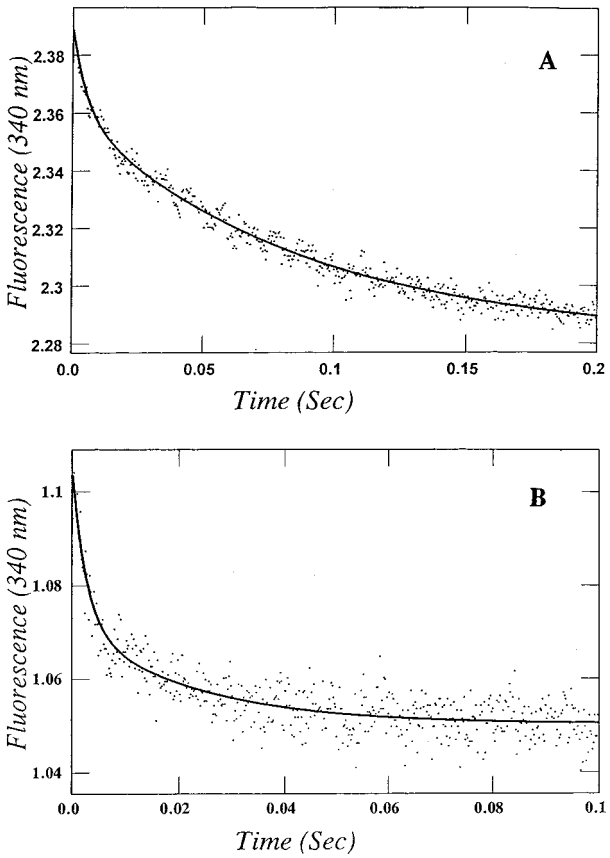

FIGURE 2: Measurement of the apparent binding rate for H_2folate binding to bifunctional TS−DHFR and *E. coli* DHFR. Representative stopped-flow fluorescence traces monitoring the decrease in intrinsic protein fluorescence as a function of time when H_2folate (5 μM) was mixed with 0.29 μM bifunctional TS−DHFR (A) or *E. coli* DHFR (B) in buffer A at 25 °C. The data for the bifunctional TS−DHFR enzyme were fit to a double exponential to provide rates of 187 ± 22 and 9 ± 0.46 s^{-1} for the fast and slow phases, respectively. For the *E. coli* DHFR enzyme, a double-exponential fit provided rates of 375 ± 60 and 44 ± 6 s^{-1} for the fast and slow phases, respectively.

Scheme 2

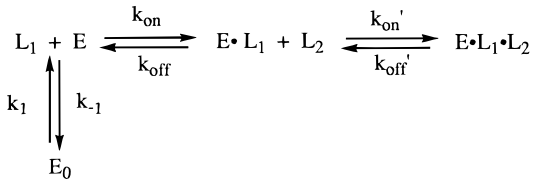

slope of the linear plot of k_{obs} versus [L]. A representative plot of k_{obs} versus [L] in the ligand-dependent phase is shown in Figure 3 for the binding of H_2folate to TS−DHFR. Accordingly, the binding rate constant for H_2folate for formation of the binary complex with the TS−DHFR bifunctional enzyme is 21 μM^{-1} s^{-1} at 25 °C and pH 7.8 (buffer A). The association rate constants measured for the various complexes between the ligand and the DHFR domain of bifunctional TS−DHFR are summarized in Table 2. These binding rate constants are similar to those reported for the *E. coli* monofunctional DHFR (*4*).

In an experiment designed to determine the rate constant for the binding of H_4folate to the bifunctional TS−DHFR enzyme, only a single slow phase was observed which had a rate of 9 ± 0.5 s^{-1}. Since this rate was independent of

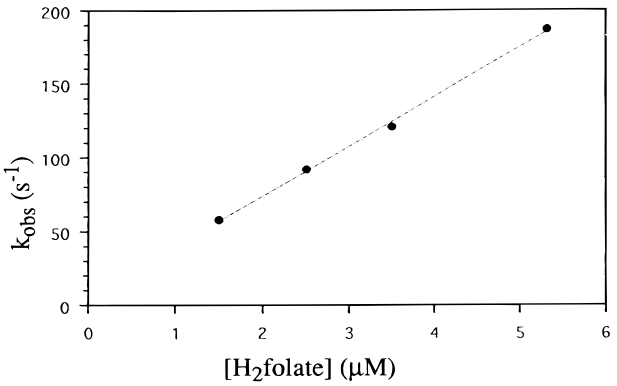

FIGURE 3: Determination of the association rate constant for H_2folate binding to bifunctional TS−DHFR. The concentration dependence of the rate of H_2folate binding to enzyme was determined by mixing TS−DHFR (0.29 μM) with H_2folate (1.5−5 μM) at pH 7.8 and 25 °C. The rate of the faster phase was fit to a line having a slope of 21 μM^{-1} s^{-1} which is the second-order rate constant for H_2folate binding to the enzyme.

Table 2: Kinetics of Association for the DHFR Site of TS−DHFR at pH 7.8 and 25 °C

ligand	enzyme species	k_{on} (μM^{-1} s^{-1})
H_2folate	E	34 ± 1
NADPH	E	21 ± 1
NADPH	E·H_4folate	20 ± 2
H_4folate	E	9 ± 0.5 s^{-1} [a]
$NADP^+$	E·H_4folate	47 ± 2
$NADP^+$	E	21 ± 1

[a] This rate constant is independent of ligand concentration and therefore first-order; see the text for an explanation.

Scheme 3

$$E\bullet L_1 \underset{k_1}{\overset{k_{-1}}{\rightleftharpoons}} E + L_1$$

$$E + L_2 \underset{k_{-2}}{\overset{k_2}{\rightleftharpoons}} E\bullet L_2$$

ligand concentration, the data indicate that a conformational change is also associated with H_4folate binding. A faster phase which is dependent upon ligand concentration may not be observable if the rate is too fast to measure and thus limited by the dead time of the stopped-flow apparatus (1.5 ms). This suggestion is supported by estimating the k_{on} (181 μM^{-1} s^{-1}) for binding from the measurements for K_d (0.016 μM) and k_{off} (2.9 s^{-1}) (Tables 1 and 3). For example, a H_4-folate concentration of 5 μM would correspond to a k_{obs} of >900 s^{-1} (181 μM^{-1} s^{-1} × 5 μM = 905 s^{-1}). Conducting the experiment at a lower H_4folate concentration (and proportionally lower enzyme concentration) to provide a slower rate was not feasible as the intrinsic protein fluorescence was not observable. Nonetheless, the data clearly indicate that an enzyme conformational change is associated with the binding of H_4folate.

Kinetics of Ligand Dissociation. The rate constant for the dissociation of ligands from the DHFR active site of bifunctional TS−DHFR can be measured by competition experiments (Scheme 3) as previously described (*4*). Dissociation rate constants for the release of H_4folate and $NADP^+$ from the DHFR active site of TS−DHFR were determined using this technique. As an example, the enzyme binary complex with H_4folate was mixed with a large excess of MTX which occupies the DHFR site after H_4folate is released from the binding site. Due to the different extents of protein fluorescence quenching by H_4folate and MTX, the exponential decay of the fluorescence was observed. When $k_1[L_1] \ll k_2[L_2] \gg k_{-1}$, k_{obs} for this reaction is equal to dissociation constant k_{-1} for L_1. The dissociation rate constants determined from the competition experiments at 25 °C and pH 7.8 are summarized in Table 3. The dissociation rate constants for H_4folate released from the E·H_4folate binary complex, the E·$NADP^+$·H_4folate ternary complex, and the E·NADPH·H_4folate ternary complex were measured to be 2.9, 10.9, and 66.5 s^{-1}, respectively, at pH 7.8 and 25 °C (buffer A). A representative stopped-flow fluorescence trace for the measurement of the dissociation constant of H_4folate from the E·NADPH·H_4folate ternary complex is shown in Figure 4. The rate of H_4folate release from E·NADPH·H_4folate is the fastest among the above three product complexes examined. It was surprising that the dissociation rate (66.5 s^{-1}) of H_4folate from E·NADPH·H_4-folate in the case of the *Leishmania* TS−DHFR bifunctional enzyme is much faster than the value of 12 ± 2 s^{-1} measured for the monofunctional *E. coli* DHFR under the same conditions (*4*). To account for any differences which may be due to the buffer, the rate of H_4folate release from the E·NADPH·H_4folate ternary complex for the bifunctional TS−DHFR and monofunctional *E. coli* DHFR enzymes was also determined in buffer B at pH 7.8. Using either set of conditions (buffer A or B), the rate of H_4folate release from E·NADPH·H_4folate in *Leishmania* DHFR is more than 3-fold faster than that observed for the *E. coli* DHFR. Thus, a second difference in the two enzyme is the much faster rate of product release for the bifunctional enzyme.

Table 3: Kinetics of Dissociation for the DHFR Site of TS−DHFR at pH 7.8 and 25 °C

ligand	enzyme species	trapping ligand	k_{off} (s−1)[a]
H_2folate	E·H_2folate	MTX	6.8
NADPH	E·NADPH	$NADP^+$	1.8
H_4folate	E·H_4folate	MTX	2.9
H_4folate	E·$NADP^+$·H_4folate	MTX	10.9
H_4folate	E·NADPH·H_4folate	MTX	66.5
$NADP^+$	E·$NADP^+$	NADPH	120
$NADP^+$	E·$NADP^+$·H_4folate	NADPH	127

[a] The error associated with the measurement of each rate constant is <10% in all cases.

Step Which Limits Steady-State Turnover. The rate-limiting step during steady-state turnover for the *E. coli* DHFR enzyme has been shown to be the release of H_4folate from the E·NADPH·H_4folate ternary complex (*4*). However, in the case of bifunctional TS−DHFR, this step could not be rate-limiting since the rate of dissociation (66.5 s^{-1}) is much faster than the steady-state rate (9 s^{-1}). Using the competition technique, the dissociation rate for $NADP^+$ displaced by NADPH at the DHFR site of TS−DHFR was measured to be 127 ± 8 s^{-1} at pH 7.8 and 25 °C, indicating that this step is also not rate-limiting. Our analysis of the reaction kinetics for the bifunctional TS−DHFR indicates that the steady-state rate is equal to the interconversion rate of two enzyme conformers observed from the kinetics of

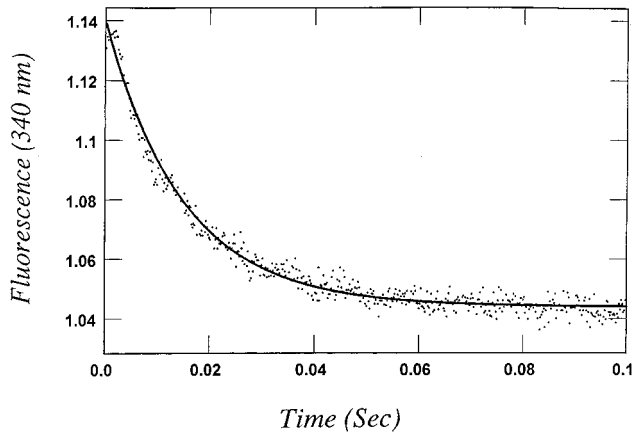

FIGURE 4: Determination of the dissociation rate constant for dissociation of H_4folate from the E·H_4folate·NADPH complex. The k_{off} rate for H_4folate dissociation from the E·H_4folate·NADPH ternary complex was measured by monitoring the decrease in intrinsic protein fluorescence after mixing a solution containing TS−DHFR (0.29 μM), NADPH (2.5 μM), and H_4folate (2.5 μM) with an excess of MTX (50 μM) at pH 7.8 and 25 °C. The data were fit to a single exponential to provide a k_{off} rate of 66.5 ± 0.9 s^{-1} for H_4folate.

binding of NADPH or H_2folate to TS−DHFR (Scheme 2). Thus, a kinetic pathway for the bifunctional TS−DHFR is suggested in which a conformational change associated with product release after formation of ternary complex E·$NADP^+$·H_4folate at the active site. It is possible that this conformational change is the step which is rate-limiting in the reaction pathway under conditions where multiple enzyme turnovers are occurring.

Identification of the Rate-Limiting Conformational Change. To more fully understand the nature of the conformational change which may limit the DHFR reaction for the bifunctional TS−DHFR under conditions of steady-state turnover, further examination was required. A summary of possible pathways for the DHFR reaction is illustrated Scheme 4 which includes the rate constants measured during the course of our studies. As shown in Scheme 4, the binding of NADPH and H_2folate leads to the formation of an E·NADPH·H_2folate complex which can undergo chemical catalysis to form E_0·$NADP^+$·H_4folate. This ternary product complex has several options (pathways 1−3) in proceeding to regenerate the E·NADPH·H_2folate substrate complex for

Scheme 4

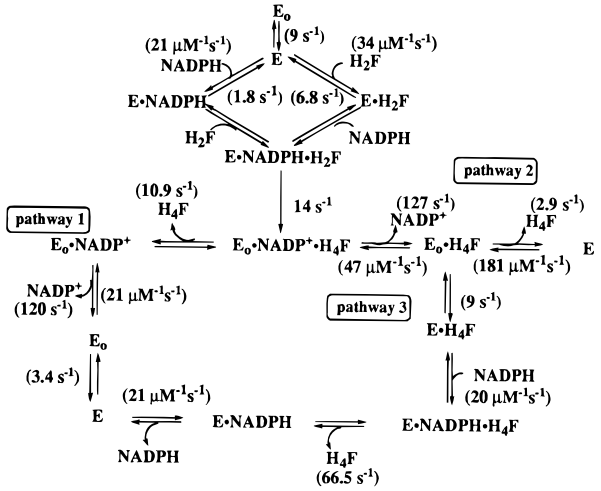

the next turnover. In pathway 1, H_4folate is first released with a rate constant of 10.9 s^{-1} as measured in this study. In pathway 2, $NADP^+$ is released first, followed by H_4folate with a rate constant of 2.9 s^{-1}. Since the rate constant for the release of H_4folate in pathway 2 is slower than the steady-state turnover rate, this pathway is ruled out. On the other hand, pathway 3 involves first the release of $NADP^+$, followed by the binding of NADPH to form an E·NADPH·H_4folate. The rate of release of H_4folate from this complex is 66.5 s^{-1} as measured in these studies. Thus, either pathway 1 or pathway 3 is plausible since the rate constants are faster than steady-state turnover. We used coenzyme energy transfer experiments to distinguish between pathway 1 and pathway 3 and to discern the most likely pathway taken to regenerate the E·NADPH·H_2folate substrate complex for multiple turnovers. This approach offers the advantage of measuring not only NADPH binding rates but also changes in enzyme conformation which may occur as a result of a relative change in orientation of NADPH at the active site. As shown in Figure 5A, the conformational change which is observed when the NADPH displaces $NADP^+$ from E_0·H_4folate (pathway 3) is biphasic and occurs at rates of 118 ± 7 and 9 ± 0.5 s^{-1}. The rate of the slower phase is approximately equal to the steady-state rate. In a separate experiment, the enzyme and H_4folate were mixed with NADPH in the absence of $NADP^+$. Under these conditions, a single fast phase was observed in which the rate was 114 ± 1.2 s^{-1} (Figure 5B). A third experiment was performed in which the rate of $NADP^+$ release was determined in the absence of H_4folate as indicated in pathway 1 in which H_4folate is released first. As shown in Figure 5C, the data were biphasic with the faster phase occurring at a rate of 42 ± 2.5 s^{-1} and the slower phase corresponding to a rate of 3.4 ± 0.05 s^{-1}. In separate experiments, we have measured the rate of the faster phase on a shorter time scale to more accurately define the rate. Under these conditions, the rate of the fast phase is 120 ± 2.5 s^{-1}. Since the rate of the slower phase (3.4 s^{-1}) is slower than the steady-state rate, the reaction scheme shown in pathway 1 is unlikely.

Taken together, the data in panels A−C of Figure 5 support pathway 3 as the preferred kinetic pathway for multiple enzyme turnovers. As summarized in Scheme 5, the kinetically preferred reaction pathway involves a slower step which may represent a conformational change associated with the release of $NADP^+$ (E_0·H_4folate to E·H_4folate). Moreover, since the rate of this conformational change is equal to the steady-state rate, it is likely that this is the step which limits the overall DHFR turnover rate for the bifunctional TS−DHFR enzyme. The E·NADPH·H_4folate complex which is formed after the conformational change and the binding of NADPH can release H_4folate. This allows the E·NADPH complex to take up another molecule of H_2-folate to regenerate the substrate complex for catalysis.

Chemical Catalysis under Multiturnover Conditions. Single-turnover experiments using rapid chemical quench methods have previously been used to determine the rate of chemical catalysis which was 14 ± 2 s^{-1}. Coenzyme fluorescence energy transfer experiments were used to measure the rate of H_4folate formation from H_2folate under conditions of multiple enzyme turnovers. A representative stopped-flow fluorescence trace is shown in Figure 6. In this experiment, the bifunctional TS−DHFR enzyme (7.5

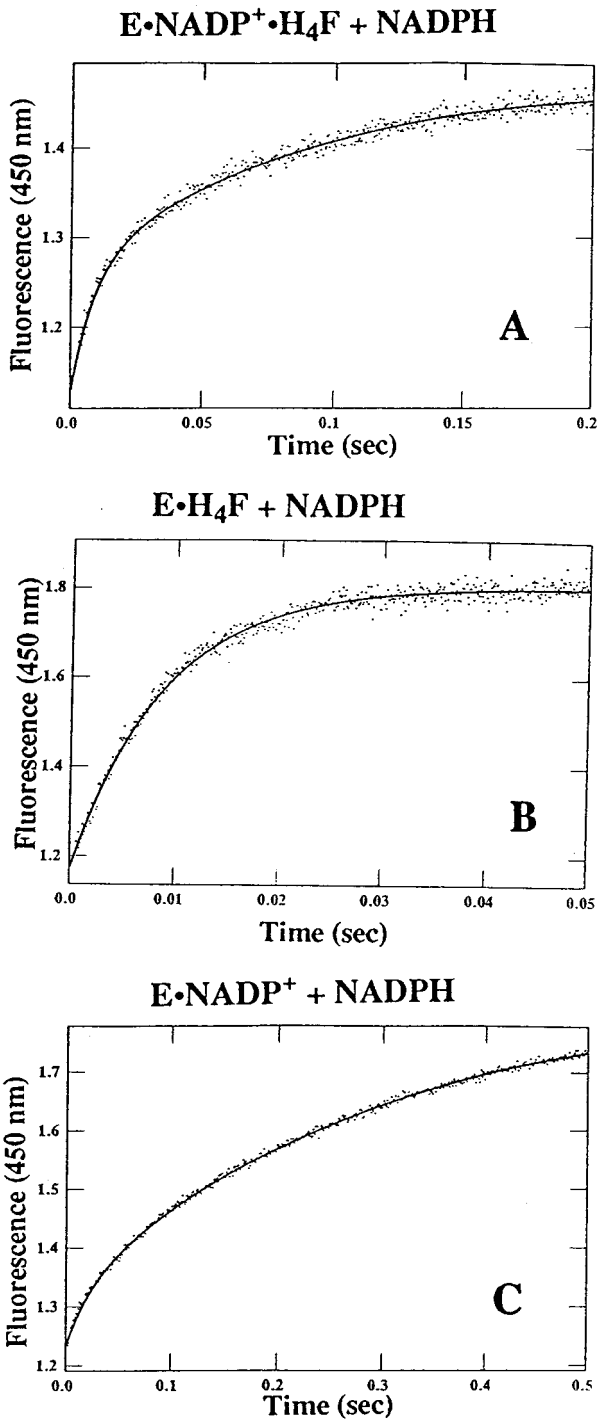

FIGURE 5: Determination of the $NADP^+$ release rate and conformational change using coenzyme fluorescence energy transfer. (A) Representative stopped-flow fluorescence trace when TS−DHFR (0.29 μM) preincubated with H_4folate (2.5 μM) and $NADP^+$ (5 μM) was mixed with NADPH (10 μM). The data were fit to a double exponential to give rates of 118 ± 7 and 9 ± 0.5 s^{-1} for the faster and slower phases, respectively. (B) Representative stopped-flow fluorescence trace when TS−DHFR (0.29 μM) preincubated with H_4folate (2.5 μM) was mixed with NADPH (10 μM). The data were fit to a single exponential with a rate of 114 ± 1.2 s^{-1}. (C) Representative stopped-flow fluorescence trace when TS−DHFR (0.29 μM) preincubated with $NADP^+$ (5 μM) was mixed with NADPH (10 μM). The data were fit to a double exponential to give rates of 42 ± 2.5 and 3.4 ± 0.05 s^{-1} for the faster and slower phases, respectively. As indicated in the text, experiments examining the faster phase on a shorter time scale provided a more accurate rate of 120 ± 2.5 s^{-1}.

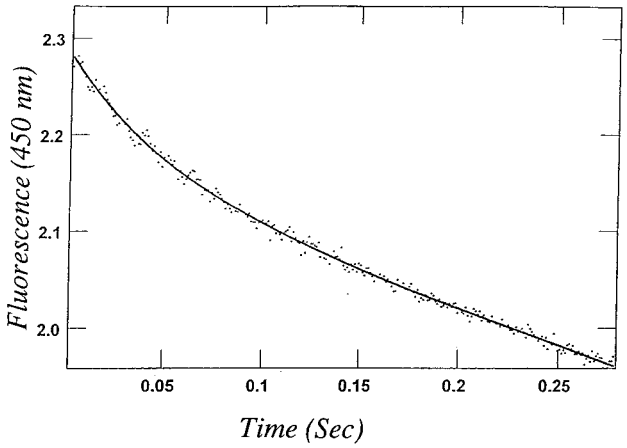

FIGURE 6: Conversion of NADPH to $NADP^+$ as measured by coenzyme fluorescence energy transfer. A representative stopped-flow fluorescence trace shows the time-dependent formation of $NADP^+$ after mixing a solution of bifunctional TS−DHFR (7.5 μM) preincubated with NADPH (500 μM) with H_2folate (500 μM) in buffer A at pH 7.8 and 25 °C. The data were fit to a burst equation with rates of 14 ± 0.8 and 9 ± 0.6 s^{-1} for the faster and slower phases, respectively. The similarity in the rates most likely indicates that the chemical step rate constant is very close to the rate constant for the conformational change at pH 7.8.

Scheme 5: *Leishmania* Bifunctional DHFR Reaction Pathway

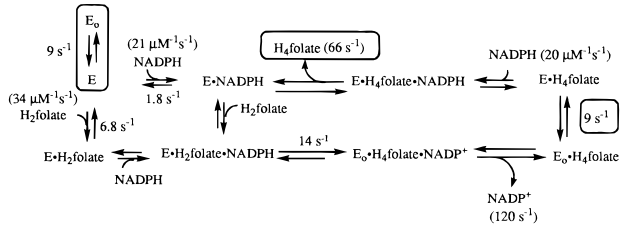

μM) was preincubated with a saturating concentration of NADPH (500 μM) and then mixed with a saturating concentration of H_2folate (500 μM) at pH 7.8. A burst product formation of product is observed with a faster chemical step rate (14 ± 0.8 s^{-1}) followed by a slower steady-state rate (9 ± 0.6 s^{-1}). At pH 7.8, the rate constants of the chemical step and conformational changes are very close. Since previous studies with the monofunctional *E. coli* DHFR enzyme (*4*) have shown that the chemical step represents hydride transfer, the rate of the chemical step would be faster at a lower pH. Thus, when we conducted the same experiment described above at pH 6.5 (data not shown) with the bifunctional TS−DHFR enzyme, a burst of product formation was observed with a faster phase of 289 ± 20 s^{-1} and a slower linear phase with a rate of 8 ± 1 s^{-1}. These results lend support to the suggestion that it is a conformational change and not the chemistry step which is rate-limiting.

Thus, as indicated above, the steady-state rate is determined by a conformational change associated with the displacement of $NADP^+$ from the E_0•$NADP^+$•H_4folate complex by NADPH. This rate-limiting step occurs after chemical catalysis (hydride transfer) in the *Leishmania* TS−DHFR bifunctional enzyme and predicts the burst of product formation under multiple-turnover conditions (excess substrate over enzyme) shown in Figure 6.

A Comparison of Monofunctional DHFR and Bifunctional TS−DHFR. A summary of the DHFR kinetic pathway for

the bifunctional enzyme is shown in Scheme 5. Under steady-state kinetic conditions, *Leishmania* bifunctional TS−DHFR and *E. coli* DHFR show similar kinetic behavior. Both enzymes display similar steady-state rates (9 s^{-1} for *Leishmania* TS−DHFR vs 12 s^{-1} *E. coli* DHFR at pH 7.8). The points in the kinetic reaction pathway for bifunctional TS−DHFR which differ from those of the monofunctional enzyme are highlighted in boxes (Scheme 5). For instance, the *Leishmania* TS−DHFR has a 3-fold higher rate of product release as compared with the *E. coli* DHFR. More importantly, the two enzymes differ in the rate-limiting step at neutral pH. The apparent pK_a observed for *E. coli* DHFR is due to a change in the rate-limiting step from product release at low pH to hydride transfer above pH 8.4. However, at low and neutral pH, the rate-limiting step in the reaction pathways of *Leishmania* bifunctional TS−DHFR is a conformational change associated with $NADP^+$ release. This conformational change is observed to be 5-fold slower for the bifunctional enzyme as compared with the *E. coli* DHFR. The difference in this rate-limiting step of these two enzymes is undoubtedly complex but may be related to several contributing factors such as interdomain interactions in the bifunctional enzyme, protein shape and size, or intrinsic structural differences within the DHFR domains. While conformational changes in the monofunctional DHFR enzymes are well-documented (*2*, *4*, *20*), an understanding of the conformational behavior and the impact on the kinetics in the bifunctional enzyme is just emerging.

The most important conclusion from these studies is that are several differences between the monofunctional and bifunctional enzymes that may represent crucial points of exploitation in terms of designing inhibitors which would be selective for the bifunctional TS−DHFR enzyme. In the previous report, we have shown that the bifunctional TS−DHFR enzyme exhibits substrate channeling of H_2folate and that there are domain−domain interactions which govern this process (*21*). Since the monofunctional DHFR enzyme lacks the channeling step, inhibitors which selectively interfere with substrate channeling in the bifunctional TS−DHFR enzyme may represent an additional strategy. The mechanistic information presented may serve as a basis for the design of novel antiparasitic drugs for the treatment of opportunistic infections in AIDS patients.

REFERENCES

1. Stone, S. R., and Morrison, J. F. (1982) *Biochemistry 21*, 3757−3765.
2. Stone, S. R., and Morrison, J. F. (1984) *Biochemistry 23*, 2753−2758.
3. Cayley, P. J., Dunn, S. M. J., and King, R. W. (1981) *Biochemistry 20*, 874−879.
4. Fierke, C. A., Johnson, K. A., and Benkovic, S. J. (1987) *Biochemistry 26*, 4085−4092.
5. Meek, T. D., Garvey, E. P., and Santi, D. V. (1985) *Biochemistry 24*, 678−686.
6. Ivanetich, K. M., and Santi, D. V. (1990) *FASEB J. 4*, 1591−1597.
7. Beverly, S. M., Ellenberg, T. E., and Cordingley, J. S. (1986) *Proc. Natl. Acad. Sci. U.S.A. 83*, 2584−2588.
8. Appleman, J., Beard, W., Delcamp, T., Prendergast, N., Freisheim, J., and Blakley, R. (1990) *J. Biol. Chem. 265*, 2740−2748.
9. Stroud, R. M. (1994) *Nat. Struct. Biol. 1*, 131−134.
10. Knighton, D. R., Kan, C.-C., Howland, E., Janson, C. A., Hostomska, Z., Welsh, K. M., and Matthews, D. A. (1994) *Nat. Struct. Biol. 1*, 186−194.
11. Grumont, R., Washtien, W. L., Caput, D., and Santi, D. V. (1986) *Proc. Natl. Acad. Sci. 83*, 5387−5391.
12. Grumont, R., Sirawaparaport, W., and Santi, D. V. (1988) *Biochemistry 27*, 3776−3784.
13. Blakley, R. L. (1960) *Nature 188*, 231−232.
14. Mathews, C. K., and Huennekens, F. M. (1960) *J. Biol. Chem. 235*, 3304−3308.
15. Curthoys, H. P., Scott, J. M., and Rabinowitz, J. C. (1972) *J. Biol. Chem. 247*, 1959−1964.
16. Dawson, R. M. C., Elliott, D. C., Elliott, W. H., and Jones, K. M. (1969) *Data for Biochemical Research*, Oxford University Press, Oxford, U.K.
17. Kallen, R. G., and Jencks, W. P. (1966) *J. Biol. Chem. 241*, 5845−5850.
18. Anderson, K. S., Sikorski, J., and Johnson, K. (1988) *Biochemistry 27*, 1604−1610.
19. Johnson, K. A. (1992) *Enzymes 20*, 1−61.
20. Howell, E. E., Villafranca, J. E., Warren, M. S., Oatley, S. J., and Kraut, J. (1986) *Science 231*, 1123−1128.
21. Liang, P. H., and Anderson, K. S. (1998) *Biochemistry 37*, 12195−12205.
22. Ronald, A. R. (1996) in *Opportunistic Complications of HIV 5*, 81−107.
23. Roos, D. S. (1993) *J. Biol. Chem. 268*, 6269−6280.
24. Vasquez, J. R., Gooze, L., Kim, K., Gut, J., Petersen, C., and Nelson, R. G. (1996) *Mol. Biochem. Parasitol. 79*, 153−165.

BI9803170